Original article

Textile Research Journal
83(9) 947–960

DOI: 10.1177/0040517512464297
trj.sagepub.com

Quality and uniformity control of fiber web by roller card system. Part II: Design and validation of a roller card control system

Chung-Feng Jeffrey Kuo[1], Huy Quang Vu[1] and Yu-Ching Li[2]

Abstract

Thin web is produced from flocks of raw fiber after being processed by a carding system. In the conventional carding machine, the multi-roller design of the system has dynamic characteristic of time delay, and the quality of web output evenness is affected by the control methods. Based on the new mathematical model of a carding machine, this paper employed a new carding control system and fiber optic sensor to establish a new carding control system. The proposed improved model predictive controller is developed to solve the problem of time delay in the roller carding system using a discrete state and linear quadratic objective function, in order to minimize the deviation between predictive output and given target value. The designed controller is compared with the proportional plus integral (PI) controller based on the conventional control theories and state feedback integral controller using modern control theories as well. In experimental verification, the fiber optic sensor is installed to measure web output at the doffer, a feeding roller is controlled to change the feeding of raw cotton. The results confirm that the proposed improved model predictive controller can be provided not only to enable the output response reach the control objects also improve the production efficiency of the carding machine and enhance the web output evenness.

Keywords

roller card system, PC base controller, delay time model, photo sensor

The main purpose of a carding machine is to separate the flock of fiber such as polypropylene, cotton, or regenerated fiber to make uniform one or multi-layer web. To increase the quantity and quality of the product web, a lot of proposed approaches and inventions have been introduced by scientists and engineers and focused on two main parts: the mechanism and the control system. In 1964, Higuchi and Takahashi[1] found the mathematical model of the roller set for the transfer function of the roller carding system, employed the final value theorem and the power spectrum density to analyze and obtain the delay time and time constant, and investigated the effect of four types of system controllers on the delay time and external interference. In 1991, Fritzsche[2] proposed a spacing sensor and check the spacing between the main carding cylinders and carding machine parts such as licker-in, stationary flat, doffering roller. Faas et al.[3] also introduced a drum of the carding machine made from fiber-reinforced synthetic material. Although it has smaller diameter, it is operated at the same or a somewhat higher circumferential speed in comparison with a conventional card. In 2001, Kuo and Hsieh[4] analyzed the

[1]National Taiwan University of Science and Technology - Department of Materials Science & Engineering, Taipei, Taiwan
[2]National Taiwan University of Science and Technology - Graduate Institute of Automation & Control, Taipei, Taiwan

Corresponding author:
Chung-Feng Jeffrey Kuo, National Taiwan University of Science and Technology - Department of Materials Science & Engineering, 43, Keelung Road, Section 4, Taipei 106, Taiwan.
Email: jeffreykuo@mail.ntust.edu.tw

dynamic model for the roller carding system, and utilized the back propagation neural network to design the controller, in order to control the yarn quality and evenness and improve the transient response. Guo et al.[5] introduced a control system using the generalized predictive control theory in 2003. In 2009, Schlichter and Vollrath[6] developed an approach related to a roller for fiber processing machine as the flat card or roller card to improve uniform of carding nip on the processing roller by using the complex roller including at least one metal cylinder and one sheath of fiber-reinforced plastics material surrounding the cylinder. While, Bradley and Edward[7] presented a new invention to produce multi-layer web product with high performance from long fiber and short fiber that can reduce the processing and material cost. In 2006, to improve the quality of card processing, Schmid and Wust[8] developed a new lick-in system with three rollers, the first two rollers have the same diameters, the third roller closed to the main cylinder has larger diameter. Pinto[9] designed a carding machine adapted for maintaining low fiber density on the main finish roller during increasing production rate of the machine through the discharge of a certain amount of fully opened fibers from the breaker or first cylinder and thus increase in productivity and reduce the carding cost. In addition, there still exist some problems of the carding system due to the characteristics of the system, namely, nonlinearity and high-order dynamic changes. The nonlinearity is the result of time delay in the carding process. When the input of a feeding roller is changed, the doffer's output will reflect the effect of the change in the input on the output after some time delay. The length of delay time is correlated with the setting of the carding machine, roller set and transfer rate of cotton web.

This paper is the second part of the research series 'Quality and uniformity control of fiber web by roller card system'. In the first part, 'Dynamic modeling formulation and experimental identification', we proposed a new mathematical model for the roller carding machine. As for system analysis, it is divided into three parts: feed input, main carding, and doffer output. The system input is the mass flow rate of fiber web per unit area. First, the mathematical model of each part can be obtained based on the principle operation and the structure of mechanism, and then the mathematical model of the entire roller card system is derived by integrating the aforementioned three parts. Experiments were conducted one real carding machine to confirm the quality of the new proposed model. In the second part, we focus on developing two modern controllers: one is designed based on the state space feedback controller with integrator and another is the discrete model predictive controller. Model predictive control (MPC) is one of the optimum control techniques, thus it can help to solve complex systems and processes, the systems with multiple inputs and outputs, as well as problems with optimum multiple standards by using the object function.[10,11] Therefore, it is capable of effectively solving the problem of time delay in the carding machine, and utilizes the quadratic performance index with minimum deviation between predictive output and given value. Experiments are carried out with three different controllers including above two controllers and PI controller and compared the output performances of these controllers through the obtained variation coefficients.

Mathematic model of carding machine

A carding machine usually includes some main subsystems such as a feed roller, taker-in (licker-in), main cylinder, flat card or roller card (worker-stripper), and doffer roller system. A typical carding machine with one card with three tripper-worker subsystems is described as in Figure 1.

The mathematic modeling model of this carding machine is described as follows:[12]

$$\begin{aligned} Q_o(t) &= (1-\eta_w)k_1k_2k_d\eta_d\frac{n\pi r_{t1}}{v_{t1}}S_fV_f \\ &\quad \times (t-\tau_{t1}-\tau_{t2}-\tau_\theta-\tau_{senser}-\tau_d)[1-e^{-kt}] \\ &= (1-\eta_w)k_1k_2k_d\eta_d\frac{n\pi r_{t1}}{v_{t1}}S_fV_f(t-T)[1-e^{-kt}] \end{aligned} \quad (1)$$

where τ_{t1} is the delayed time of the feeding roll with the first take-in roll, τ_{t2} is the time delayed from the first take-in roll to the second take-in roll, τ_θ is the angle created by the contact points between the take-in roll with cylinder and the work roll with cylinder, τ_{sensor} is calculated by measuring the time of fiber web output flowing to the optic sensor system, T is the total time delay, τ_d is the time passing of fiber from the contact point between the cylinder with doffer input to the fiber web output, S_f is the fiber count; V_f is the speed of the feed roller, k_1 is the attenuation factor between the first take-in and the second take-in, k_2 is the attenuation factor between the second take-in and cylinder, and k is the ratio constant between $Q_{c2}(t)$ the mass flow rate of cylinder output and $Q_d(t)$ the mass flow rare input of doffer, η_w is the collecting power of fibers through the first contact point on the cylinder, n is the revolutions per minute of the first take-in roll, k_d is the attention factor between the input and output of doffer, η_d is the collecting power of fibers through the first contact point on the doffer, and $Q_o(t)$ is the mass flow rate of the fiber web output.

According to our previous work,[12] after applying the Laplace transform and the time delay functions, the

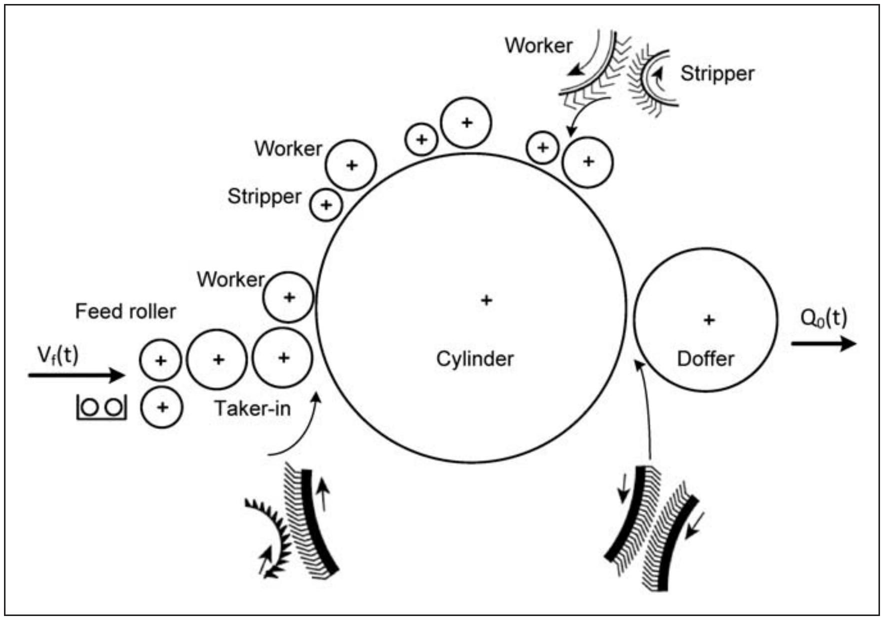

Figure 1. The scheme of a carding machine.

open-loop transfer function of the whole carding machine system can be obtained as follows:

$$\frac{Q_o(s)}{V_f(s)} = (1 - \eta_{w1})k_1 k_2 k_d \eta_d \frac{n\pi r_{t1} S_f}{v_{t1}} \frac{\left[(1 - \frac{1}{e^{kT}})s + k\right]}{Ts^2 + (Tk + 1)s + k} \tag{2}$$

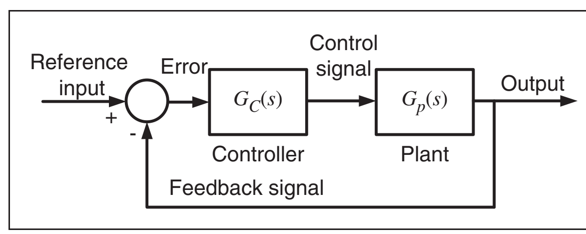

Figure 2. Block diagram of the feedback control system.

Controller design

Classical and modern control theories

As shown in Figure 2, the basic design technique of the classical control system is to apply one group of blocks of compensable original system in the feedback path. These blocks are expressed by the transfer functions $G_C(s)$ of the controller and $G_p(s)$ of the plant (system). The design technique based on parameter damping ratio ξ and un-damped nature frequency ω_n provides these blocks with the actions and functions of the regulator, so they are called controllers. Output feedback is used to make the regulating parameters of the controller meeting the required transient performance and eliminating steady-state error. The controller device of the carding machine in this study first designs a PI controller to improve web density and remove the steady-state error of the uneven fragments.

Based on the modern control theories, the mathematical model of the dynamic system is expressed by the state feedback model. The one-order differential equation of one group of state variables is used to describe the system. The method can be utilized to analyze the multi-input and multi-output system, as the dynamic equation can be expressed in matrix form. Therefore, it is particularly applicable to the computer software for control and calculation. As shown in Figure 3, the main design technique in the modern control system is based on the state feedback control principle, whose main framework is that the state variables undergo fixed real number increment gain K feedback and produce suitable control signals to improve the dynamic performance. Lastly, based on the state feedback control principle, this study will propose a state feedback with integral control to manipulate web output evenness of the carding machine.

State feedback with integral control

The structure, as shown in Figure 4, is from output y feedback to the general junction point, and produces an error signal, $\dot{\xi}$, with the unit step reference input. The error signal enters the feedback control system through the integrator.[13]

This state feedback is under integral control of steady-state error design, which increases the system type. The dynamic mode of unit step reference command introduced into the integrator is $1/s$. The design mode is called the interior model design. The output of the integrator may be defined as the state variable ξ, and the differential of state variable $\dot{\xi}$ defined as follows:

$$\dot{\xi} = r - y = r - Cx \tag{3}$$

The state equation of the system is as follows:

$$\dot{x} = Ax + Bu \tag{4}$$

$$y = Cx \tag{5}$$

where u is the control signal (scalar), y is the output signal (scalar), and r is the reference input signal.

The control signal u may change the system state variable after state feedback of constant gain and output feedback with integral control, and it is expressed as follows:

$$u = -Kx + K_I\xi \tag{6}$$

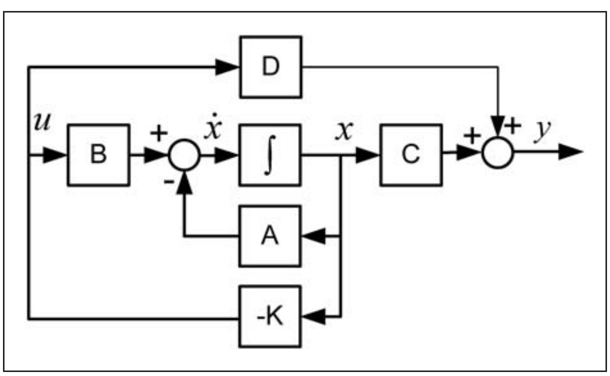

Figure 3. Block diagram of a carding machine with state feedback.

Equations (3) and (4) can be expressed by the matrix form of the augmented state:

$$\begin{bmatrix} \dot{x}(t) \\ \dot{\xi}(t) \end{bmatrix} = \begin{bmatrix} A & 0 \\ -C & 0 \end{bmatrix} \begin{bmatrix} x \\ \xi \end{bmatrix} + \begin{bmatrix} B \\ 0 \end{bmatrix} u(t) + \begin{bmatrix} 0 \\ 1 \end{bmatrix} r(t) \tag{7}$$

$$y = \begin{bmatrix} C & 0 \end{bmatrix} \begin{bmatrix} x \\ \xi \end{bmatrix} \tag{8}$$

An asymptotically stable control system is proposed for the carding machine and then the steady state of system $x(\infty)$ and $\xi(\infty)$ approaches a constant value that leads to

$$\dot{\xi}(t) = 0, y(\infty) = r \tag{9}$$

the steady state of the system is

$$\begin{bmatrix} \dot{x}(\infty) \\ \dot{\xi}(\infty) \end{bmatrix} = \begin{bmatrix} A & 0 \\ -C & 0 \end{bmatrix} \begin{bmatrix} x(\infty) \\ \xi(\infty) \end{bmatrix} + \begin{bmatrix} B \\ 0 \end{bmatrix} u(\infty) + \begin{bmatrix} 0 \\ 1 \end{bmatrix} r(\infty) \tag{10}$$

When the reference signal is the step input, we have

$$r(\infty) = r(t) = r \tag{11}$$

Define error states:

$$\begin{aligned} x(t) - x(\infty) &= x_e(t) \\ \xi(t) - \xi(\infty) &= \xi_e(t) \\ u(t) - u(\infty) &= u_e(t) \end{aligned} \tag{12}$$

The error states' equations can be rewritten as

$$\begin{bmatrix} \dot{x}_e(t) \\ \dot{\xi}_e(t) \end{bmatrix} = \begin{bmatrix} A & 0 \\ -C & 0 \end{bmatrix} \begin{bmatrix} x_e(t) \\ \xi_e(t) \end{bmatrix} + \begin{bmatrix} B \\ 0 \end{bmatrix} u_e(t) \tag{13}$$

Error of control signal u

$$u_e(t) = -KX_e(t) + K_I\xi_e(t) \tag{14}$$

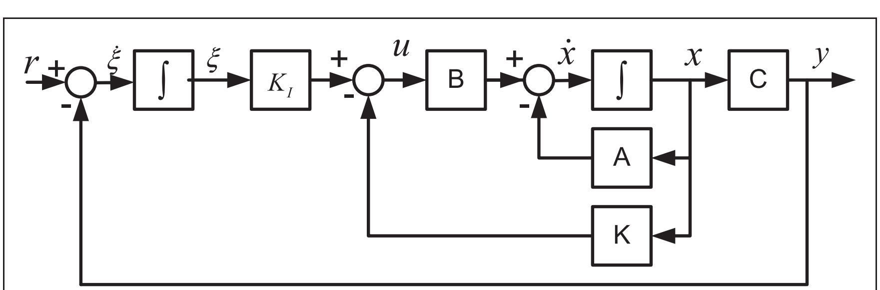

Figure 4. Block diagram of state feedback and integral output feedback.

Define error vector $e(t)$ by

$$e(t) = \begin{bmatrix} x_e(t) \\ \xi_e(t) \end{bmatrix} \tag{15}$$

Equation (13) can be rewritten as

$$\dot{e}(t) = \tilde{A}e(t) + \tilde{B}u_e(t) \tag{16}$$

where

$$\tilde{A} = \begin{bmatrix} A & 0 \\ -C & 0 \end{bmatrix}, \ \tilde{B} = \begin{bmatrix} B \\ 0 \end{bmatrix} \tag{17}$$

Equations (14) and (15) can be changed into

$$u_e(t) = -\tilde{K}e(t) \tag{18}$$

$$\tilde{K} = \begin{bmatrix} K & -K_I \end{bmatrix} \tag{19}$$

The state error equation can be obtained by substituting Equation (18) into Equation (16):

$$\dot{e}(t) = \tilde{A}e(t) - \tilde{B}\tilde{K}e(t) = (\tilde{A} - \tilde{B}\tilde{K})e(t) \tag{23}$$

Augmented matrix equation of the whole system integrating constant increment and integral control is

$$\begin{bmatrix} \dot{x}(t) \\ \dot{\xi}(t) \end{bmatrix} = \begin{bmatrix} A - BK & BK_I \\ -C & 0 \end{bmatrix} \begin{bmatrix} x(t) \\ \xi(t) \end{bmatrix} + \begin{bmatrix} 0 \\ 1 \end{bmatrix} r(t) \tag{20}$$

$$y(t) = \begin{bmatrix} C & 0 \end{bmatrix} \begin{bmatrix} x \\ \xi \end{bmatrix} + [0]r(t) \tag{21}$$

Proposed improved MPC

In all controllers derived from MPC, the algorithm strategies have the following features, as shown in Figure 5. Four main concepts of the MPC theory are described as follows:

1. The principle of MPC is based on the mathematic model of the system to predict the future output and control input.
2. Determine the size of the predictive future output N_p and the predictive control input N_c through the model of processes or plants. These predictive outputs $y(k)$, $k = 1, 2, \ldots N_P$ are determined by using the information of the current time point t (i.e. past output and input) and future control signal $u(k)$, $k = 1, 2, \ldots N_c$.
3. Future control sequence can be obtained based on an optimum principle that can be described by a determined criterion to make the response output tracking and approaching the reference trajectory r, which may be the set point or one approximate estimate. A form adopted under a determined criterion can be a quadratic function expressing the error between the predictive output signal and the predictive reference trajectory. In most cases, the effect of control output is also considered and included in the objective function.
4. Only the first predictive future element in the control input sequence is applied for the control input of the real system, and then the overall procedure for finding the minimum values of the object function is repeated. The new future output and control input are calculated for the next step.

Figure 6 shows the basic structure of model prediction. The model is utilized to predict the future output of a process or a dynamic system using the past and current output and input, as well as the future optimum control actions. The optimum actions are used to calculate the objective function, namely, the error of future path is considered and the optimum control input is applied.

A continuous model of a plant is described by ordinary differential equations

$$\dot{x}_c(t) = A_c x_c(t) + B_c u(t) \tag{22}$$

$$y(t) = C_c x_c(t) + D_c u(t) \tag{23}$$

From Equations (22) and (23) we can get the discrete state-space model:

$$x_d(k+1) = A_d x_d(k) + B_d u(k) \tag{24}$$

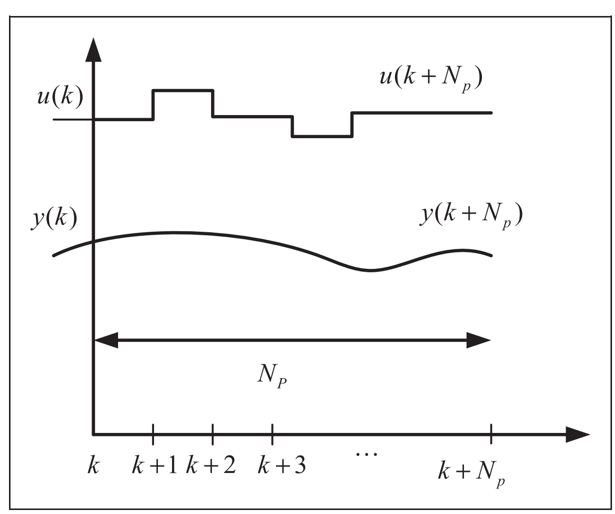

Figure 5. Strategy of model predictive control.

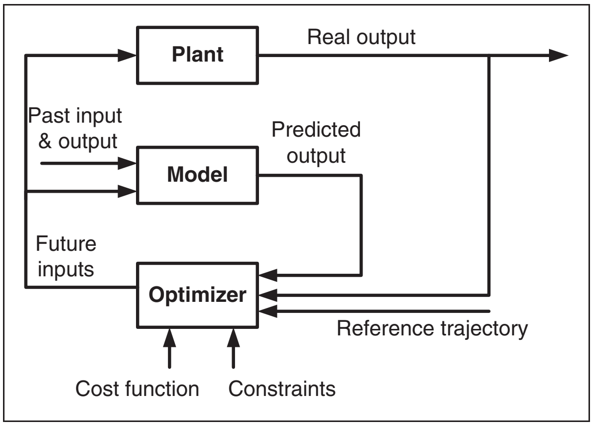

Figure 6. Basic strategies of the model predictive control system.

$$y(k) = C_d x_d(k) \tag{25}$$

The difference of the state variable and the control variable is defined as follows:

$$\Delta x_d(k) = x_d(k) - x_d(k-1) \tag{26}$$

$$\Delta u(k) = u(k) - u(k-1) \tag{27}$$

The new state-space model is defined as[4]

$$\begin{bmatrix} \Delta x_d(k+1) \\ y(k+1) \end{bmatrix} = \begin{bmatrix} A_d & O_d^{\mathrm{T}} \\ C_{\mathrm{d}} A_d & 1 \end{bmatrix} \begin{bmatrix} \Delta x_d(k) \\ y(k) \end{bmatrix} + \begin{bmatrix} B_d \\ C_d B_d \end{bmatrix} \Delta u(k) \tag{28}$$

$$y(k) = \begin{bmatrix} O_d & 1 \end{bmatrix} \begin{bmatrix} \Delta x_d(k) \\ y(k) \end{bmatrix} \tag{29}$$

or

$$x(k+1) = Ax(k) + B\Delta u(k) \tag{30}$$

$$y(k) = Cx(k) \tag{31}$$

where

$$x(k) = \begin{bmatrix} (\Delta x_d(k))^{\mathrm{T}} & y(k) \end{bmatrix}^{\mathrm{T}} \tag{32}$$

$$A = \begin{bmatrix} A_d & O_d \\ C_{\mathrm{d}} A_d & 1 \end{bmatrix} \tag{33}$$

$$B = \begin{bmatrix} B_d & C_d B_d \end{bmatrix}^{\mathrm{T}} \tag{34}$$

Suppose that the current information of the system is acquired through measurement of sampling instant time k_i,$k_i > 0$, and state variable vector $x(k_i)$.

The vectors are defined as

$$Y = \begin{bmatrix} y(k_i+1|k_i) & y(k_i+2|k_i) & y(k_i+3|k_i) \\ \ldots & y(k_i+N_p|k_i) & \end{bmatrix}^{\mathrm{T}} \tag{35}$$

$$\Delta U = \begin{bmatrix} \Delta u(k_i) & \Delta u(k_i+1) & \Delta u(k_i+2) \\ \ldots & \Delta u(k_i+N_c-1) & \end{bmatrix}^{\mathrm{T}} \tag{36}$$

In the single input and single output, the dimension of Y is N_p, and the dimension of ΔU is N_c; here N_p is the predictive time domain and N_c is the control time domain.

Based on the new state-space model, also called the augmented model, the future state variables are calculated sequentially using the set of future control parameters. In general, $N_c \le N_p$, the information derived from current state $x(k_i)$ of the system can be used to predict $x(k_i+j|k_i)$ state.

The future state variables by iteration according to predictive time domain N_p are

$$\begin{aligned} x(k_i+N_p|k_i) = {} & A^{N_p} x(k_i) + A^{N_p-1} B\Delta u(k_i) \\ & + A^{N_p-2} B\Delta u(k_i+1) \\ & + \cdots + A^{N_p-N_c} B\Delta u(k_i+N_c-1) \end{aligned} \tag{37}$$

Predictive output state variables are

$$\begin{aligned} y(k_i+N_p|k_i) = {} & CA^{N_p} x(k_i) + CA^{N_p-1} B\Delta u(k_i) \\ & + CA^{N_p-2} B\Delta u(k_i+1) \\ & + \cdots + CA^{N_p-N_c} B\Delta u(k_i+N_c-1) \end{aligned} \tag{38}$$

Every predictive state variable is determined upon current state $x(k_i)$ and future control state $\Delta u(k_i+j)$, $j = 0, 1, \ldots N_c - 1$.

From Equations (35)–(38), we have

$$Y = Fx(k_i) + \Phi\Delta u \tag{39}$$

where

$$F=\begin{bmatrix} CA \\ CA^2 \\ CA^3 \\ \vdots \\ CA^{N_p} \end{bmatrix} : \Phi=\begin{bmatrix} CB & 0 & 0 & \dots & 0 \\ CAB & CB & 0 & \dots & 0 \\ CA^2B & CAB & CB & \dots & 0 \\ \vdots & \vdots & \vdots & \vdots & \vdots \\ CA^{N_p-1}B & CA^{N_p-2}B & CA^{N_p-3}B & \dots & CA^{N_p-N_c}B \end{bmatrix} \tag{40}$$

Next, based on the minimization of the error between the set point signal and the output signal, an objective function can be defined. The cost function is defined as

$$\begin{aligned} J &= (R_s - Y)^{\mathrm{T}}(R_s - Y) + \Delta U^{\mathrm{T}}\overline{R}\Delta U \\ &= E^{\mathrm{T}}E + \Delta U^{\mathrm{T}}\overline{R}\Delta U \end{aligned} \tag{41}$$

$$R_s = \begin{bmatrix} 1 & 1 & \cdots & 1 \end{bmatrix}^{\mathrm{T}} r(k_i) = \overline{R}_s r(k_i) \tag{42}$$

$$\overline{R} = r_w I_{N_c \times N_c} \quad (r_w \geq 0) \tag{43}$$

where $r(k_i)$ is the reference point signal at k_i, R_s is the reference point signal, $\bar{R}$ is the diagonal matrix of the characteristics of the closed-loop system, r_w is a regulating parameter of the characteristics of the closed-loop system, $\overline{R}_s$ is the unit vector with N_p dimension, and E is the error vector to describe the errors between the predicative output and the reference input signal.

From Equations (39) and (41), we have a new cost function:

$$\begin{aligned} J= &(R_s - Fx(k_i))^{\mathrm{T}}(R_s - Fx(k_i)) - 2\Delta U^{\mathrm{T}}\Phi^{\mathrm{T}}(R_s - Fx(k_i)) \\ &+ \Delta U^{\mathrm{T}}\left(\Phi^{\mathrm{T}}\Phi + \overline{R}\right)\Delta U \end{aligned} \tag{44}$$

To find the optimum solutions for control input, the cost function J is minimized: taking the fist-order differential of the cost function J,

$$\frac{\partial J}{\partial \Delta U} = -2\Phi^{\mathrm{T}}(R_s - Fx(k_i)) + 2\left(\Phi^{\mathrm{T}}\Phi + \overline{R}\right)\Delta U \tag{45}$$

The condition for obtaining the minimum value J is described as follows:

$$\frac{\partial J}{\partial \Delta U} = 0 \tag{46}$$

From Equations (45) and (46), the obtained control signal of the optimum solution

$$\Delta U = \left(\Phi^T\Phi + \overline{R}\right)^{-1}\Phi^{\mathrm{T}}(R_s - Fx(k_i)) \tag{47}$$

Substituting Equation (42) into Equation (47), and obtain

$$\Delta U = \left(\Phi^T\Phi + \overline{R}\right)^{-1}\Phi^{\mathrm{T}}\left(\overline{R}_s r(k_i) - Fx(k_i)\right) \tag{48}$$

Based on the receding predictive horizon control theory, the first element of control vector ΔU is the incremental control value at time k_i

$$\begin{aligned} \Delta u(k_i) &= \begin{bmatrix} 1 & 0 & \cdots & 0 \end{bmatrix}\left(\Phi^{\mathrm{T}}\Phi + \overline{R}\right)^{-1}\Phi^{\mathrm{T}}\left(\overline{R}_s r(k_i) - Fx(k_i)\right) \\ &= K_y r(k_i) - K_{dmpc}x(k_i) \end{aligned} \tag{49}$$

In Equation (49), K_y is used to express the first element of $\left(\Phi^T\Phi + \overline{R}\right)^{-1}\Phi^T\overline{R}_s$ while K_{dmpc} is used to describe the first row of $\left(\Phi^T\Phi + \overline{R}\right)^{-1}\Phi^T F$ and can be rewritten as follows:

$$K_{dmpc} = \begin{bmatrix} K_x & K_y \end{bmatrix} \tag{50}$$

where K_x corresponds to the feedback gain vector related to $\Delta x_d(k)$.

The closed-loop system can be obtained by substituting Equation (49) into Equation (30):

$$x(k+1) = \left(A - BK_{dmpc}\right)x(k) + BK_y r(k) \tag{51}$$

The closed-loop system designed by discrete model predictive control can be described as shown in Figure 7, where q^{-1} describes the backward shift operator while $\frac{1}{1-q^{-1}}$ expresses the discrete-time integrator.

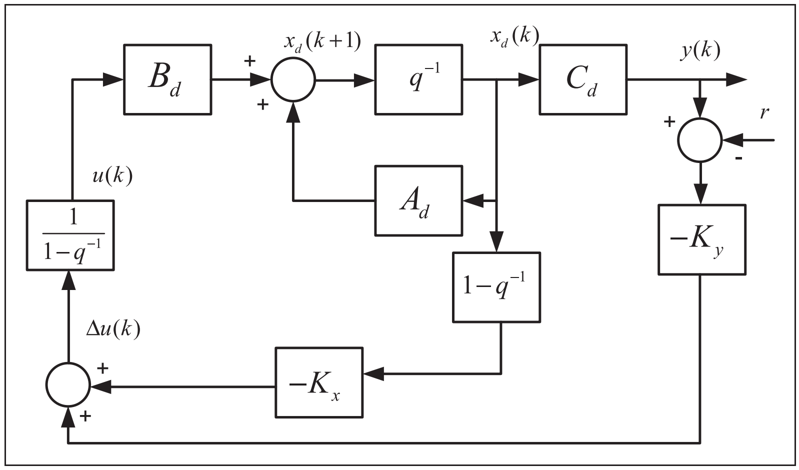

Figure 7. Scheme of discrete-time predictive control system.

Design of controllers and experiments

In the previous sections, the steps for designing generally state feedback integral controller and the discrete model predictive controller are presented in more detail. In this section we show the applications of these controllers to a real carding machine. Experiments are carried out to indicate which controller is the best for the carding machine control system. The obtained controllers are also compared with a PI controller commonly used for the carding machine in practice. The real machine includes feeding rollers, taker-in rollers, a main cylinder, a doffer roller, and three worker-stripper rollers. The physical parameters of this system are presented in Tables 1 and 2.

Hardware components

The devices which are used for experiments to confirm the proposed mathematical model have been described in detail in part one of the research series[1] and are also applied to evaluate the designed controllers.

We used a Fuji DC servo motor and driver, GYG751CC2-T2E 0.75 kw, and an infrared sensor system using optical sensor FS-V31M Keyyence (analog output 1–5 V according to the detection quantity). The minimum resolution is 0.0005 inch, equivalent to a gold wire diameter. We also used a motion control interface card RT-DAC 4/PCIm and VISSIM software.

The speed of the feed roller is controlled through a digital-to-analog converter (DAC) output (12-bit resolution and range 0–10 V) of the motion interface card RT-DAC 4/PCIm. The values of sensors output was read by analog-to-digital converter (ADC) inputs (12-bit resolution and range 0–10 V) of RT-DAC 4/PCIm. The scheme of the roller card control system is shown in detail in Figure 8.

Table 1. Parameters of each part of the roller card

Components	Radius (mm)	Velocity (rpm)
Feed roller	20	10
Take-in roller	65	98
Cylinder	190	182
Carding roller	55	10
Stripper roller	33	370
Doffer	160	10
Draft roller	310	12

From Equation (2), the open-loop transfer function of the real carding machine can be obtained as follows:

$$\frac{Q_o(s)}{V_f(s)} = \frac{0.0328s + 0.01774}{7.091s^2 + 4.758s + 0.53} \tag{52}$$

By applying the analysis of root locus analysis, suitable controller parameters are designed to conduct computer simulation of the whole system of the roller carding machine. Validation is conducted on the evenness control of online real-time web density with an actual machine.

The poles of the open-loop transfer function are in the complex left half-plane, as shown in Table 3. The system is stable. Figure 9 shows the root loci of the closed-loop system with a proportional controller.

PI controller

The control objective in this paper is that output transient response has no maximum overshoot:

$$M_{os} = e^{-\pi\xi\sqrt{1-\xi^2}} = 0, \xi = 1 \tag{53}$$

Table 2. Parameter table of the whole roller card

	τ_c	τ_w	τ_s	τ_{t1}	τ_{t2}	τ_θ	τ_{sensor}	τ_d
Delay time (sec)	0.02	4.76	0.125	0.176	0.22	0.025	0.0178	6.67
Attenuation factor	$k_1 = 1,\ k_2 = 0.311,\ k_d = 21.61$							
Collecting power	$\eta_{w1} = 0.54,\ \eta_w = 0.54, \eta_d = 0.0857$							
Transfer factor	$k = 0.53$							
Delay factor	$D = 2.02$							
Feeding speed	$V_f = 0.0137$							
Sensor gain	$k_s = 6$							
Fiber count	$S_f = 0.3355$							
Cylinder speed	$n = 25.9$ rpm							

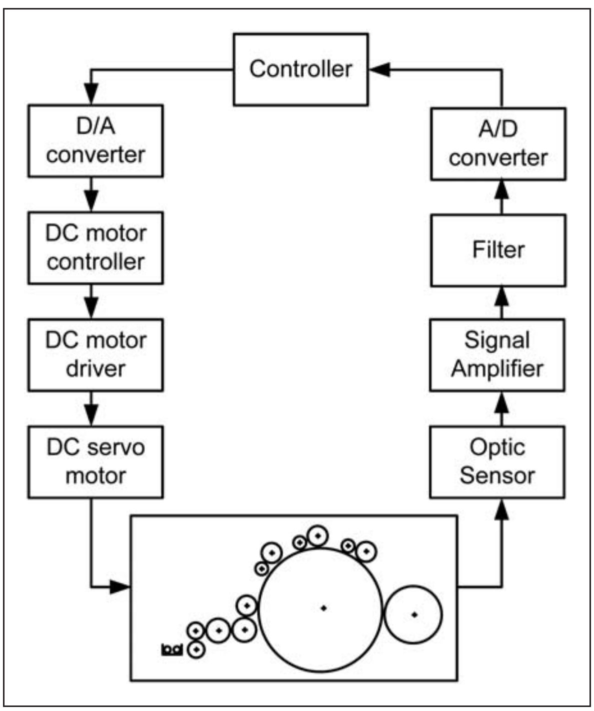

Figure 8. The scheme of a roller card control system.

Table 3. Pole–zero configurations of the roller carding machine

Poles	Zeros
−0.53	−0.54
−0.141	

The settling time is less than 20 seconds, and response output falls within 5% of the final value

$$\frac{3}{\xi\omega_n} \le 20 \Rightarrow \omega_n = 0.1 \tag{54}$$

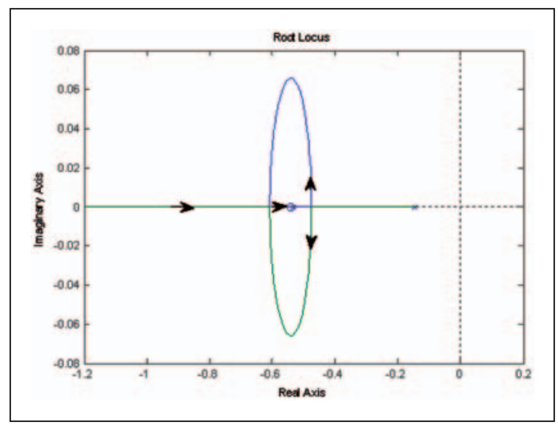

Figure 9. Root locus of the closed-loop with a proportional controller.

The setting parameters of the carding machine were: web output weight, 3.84 g; web output length, 9.734 m; cotton fiber count, 0.3945.

Suppose that the characteristic equation of the transient equation is

$$(s + a)(s^2 + 2\xi\omega_n + \omega_n^2) \tag{55}$$

Add the characteristic equation of the closed-loop transfer function of the PI controller:

$$\Delta(s) = 7.091s^3 + B(s) + C(s) + D(s) \tag{56}$$

$$B(s) = (4.76 + 0.0978k_p)s^2 \tag{57}$$

$$C(s) = (0.53 + 0.0978k_I + 0.052894k_p)s \tag{58}$$

$$D(s) = 0.052894k_I \tag{59}$$

By comparing Equation (52) with Equation (55), we obtain $a = 0.5253$ and $k_I = 4.01622$. The difference between the theoretical output and the output of

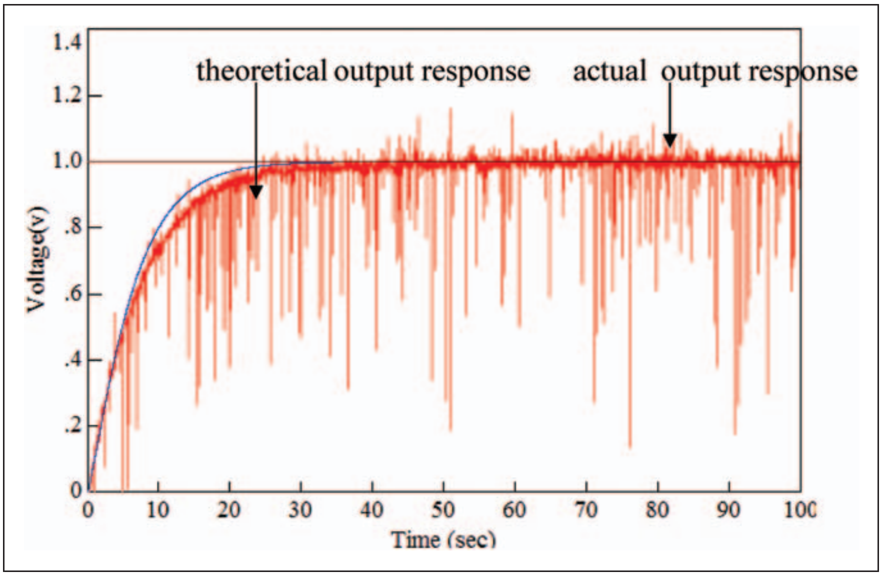

Figure 10. Comparison between the theoretical value output and actual system response with PI control added (without filter).

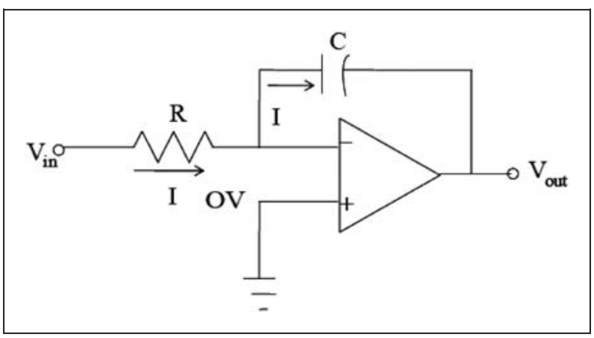

Figure 11. Low-pass integrator.

roller card control system with the added PI controller is validated and compared.

As shown in Figure 10, the output response includes sensor noise and interference produced by the motor output, the filter is utilized to remove such issues. The sensor and servomotor used in the experiment produce high-frequency noise and interference, the low-pass filter is selected to limit the high-frequency signal. Figure 11 applies the one-order low-pass filter composed of the operation amplifier.

The one-order low-pass filter circuit is also called a reversed phase integrator or Miler integrator. In this paper we selected a Butterworth filter for signal filtering, which has the smoothest amplitude at the origin of the S plane. This means that all derivatives of amplitude response at the origin are equal to zero. It includes a full-pole design, and has 3 dB attenuation characteristic at the critical frequency, so it can be used to provide the attenuation frequency and desired attenuation value. The system open-loop transfer function can be calculated through a Bode diagram, and the calculated cut-off frequency $\omega = 0.141(\text{rad/sec})$ as shown in Figure 12.

As shown in Figure 13, the output response shows that the theoretical output of the response curve of the carding system with a PI controller added is closest to the actual output, without maximum overshoot, thus satisfying the design objective of a transient response. Its coefficient of variation is 4.5178%.

State feedback with integral controller

From the obtained mathematical model of the carding system[12] as presented in Equation (2), the state space model of the system is obtained as

$$\begin{bmatrix} \dot{x}_1(t) \\ \dot{x}_2(t) \end{bmatrix} = \begin{bmatrix} -0.671 & -0.0747 \\ 1 & 0 \end{bmatrix} \begin{bmatrix} x_1(t) \\ x_2(t) \end{bmatrix} + \begin{bmatrix} 1 \\ 0 \end{bmatrix} V_f(t) \tag{60}$$

$$Q_o(t) = \begin{bmatrix} 0.0047 & 0.0025 \end{bmatrix} \begin{bmatrix} x_1(t) \\ x_2(t) \end{bmatrix} \tag{61}$$

The matrices A, B and C are

$$A = \begin{bmatrix} -0.671 & -0.0747 \\ 1 & 0 \end{bmatrix} \tag{62}$$

$$B = \begin{bmatrix} 1 \\ 0 \end{bmatrix} \tag{63}$$

$$C = \begin{bmatrix} 0.0047 & 0.0025 \end{bmatrix} \tag{64}$$

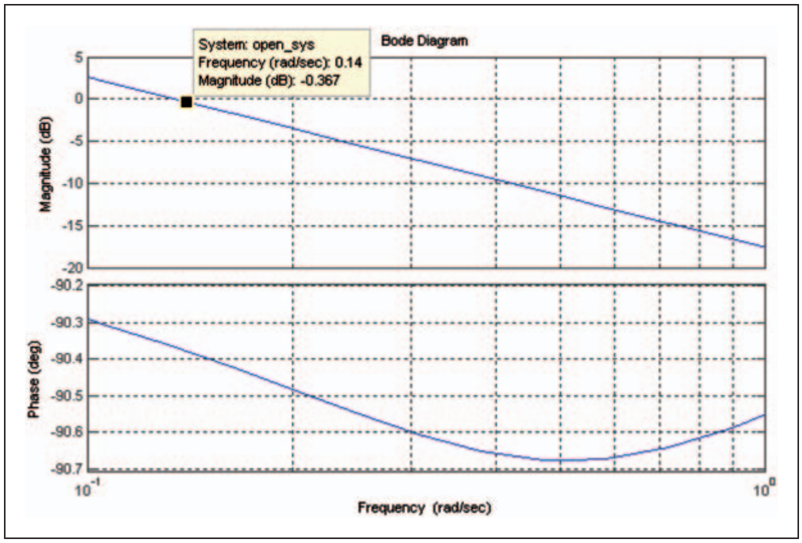

Figure 12. Expression of cut-off frequency of the transfer function of the system.

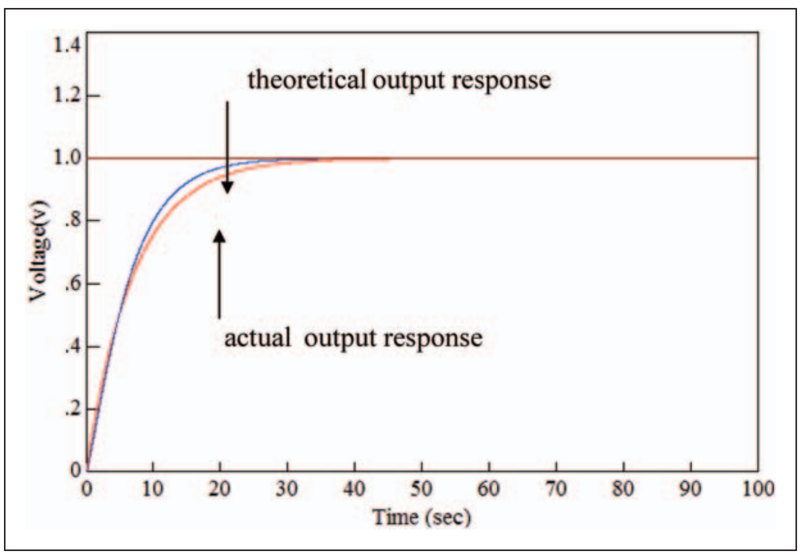

Figure 13. Comparison between theoretical output and actual output response with PI.

The controllable matrix of the system is

$$C_o = \begin{bmatrix} 1 & -0.671 \\ 0 & 1 \end{bmatrix} \quad (65)$$

The observable matrix of the system is

$$O_b = \begin{bmatrix} 0.0047 & -0.0006 \\ 0.0025 & -0.0004 \end{bmatrix} \quad (66)$$

The rank of the controllable and observable matrices can be found as follows:

$$Rank(C_o) = 2 \quad (67)$$

$$Rank(O_b) = 2 \quad (68)$$

Therefore, the system is controllable and observable.

As the system is controllable, the design is produced as follows according to the transient response specification. The settling time is less than 20 seconds, and response output falls within 5% of the final value:

$$\frac{4}{\xi \omega_n} \leq 20 \Rightarrow \omega_n = 0.2 \quad (69)$$

The design based on the pole configuration of feedback controller gives

$$\begin{bmatrix} -0.2 & -0.2 & -1 \end{bmatrix} \quad (70)$$

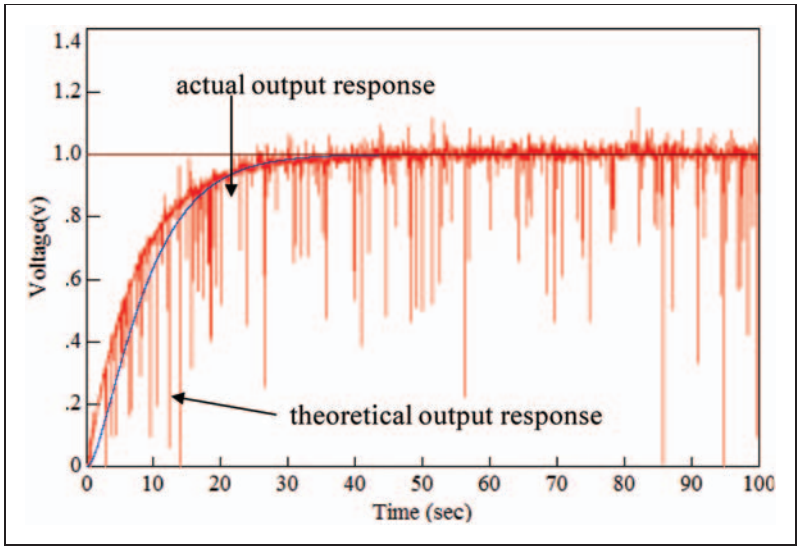

Figure 14. Response comparison between state feedback with integral control and the original system.

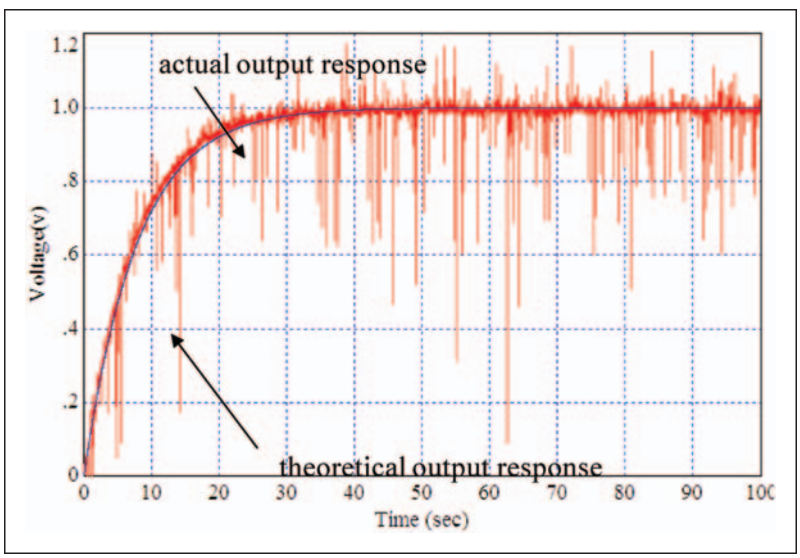

Figure 15. Compare actual output and theoretical output responses.

The characteristic equation is

$$\Delta(s) = (s + 0.2)(s + 0.2)(s + 1) \tag{71}$$

The design state feedback increment K and integral increment are

$$K = \begin{bmatrix} 0.729 & 0.2914 \end{bmatrix} \tag{72}$$

$$K_I = 15.7427 \tag{73}$$

Experimental results are presented in Figure 14. When the unit step is input, the output response of the designed state feedback with integral controller should be consistent with the response output of the actual carding machine.

Discrete model predictive controller

First, the discrete mathematical model is obtained by converting the continuous model into a discrete time system with sampling time $\Delta t = 1$:

$$x_d(k+1) = \begin{bmatrix} 0.4872 & -0.05375 \\ 0.7195 & 0.7 \end{bmatrix} x_d(k) + \begin{bmatrix} 0.7195 \\ 0.4023 \end{bmatrix} V_f(k) \tag{74}$$

Then, we find the augmented model by finding the increment state space model of state space variable and control input through Equations (22)–(34):

$$A_d = \begin{bmatrix} 0.4872 & -0.0538 \\ 0.7195 & 0.9699 \end{bmatrix} \tag{75}$$

$$B_d = \begin{bmatrix} 0.7195 \\ 0.4023 \end{bmatrix} \tag{76}$$

$$C_d = \begin{bmatrix} 0.0047 & 0.0025 \end{bmatrix} \tag{77}$$

$$D_d = [0] \tag{78}$$

Convert the discrete time system into the increment model based on Equations (28) and (29):

$$\begin{bmatrix} \Delta x_d(k+1) \\ y(k+1) \end{bmatrix} = \begin{bmatrix} 0.4872 & -0.0538 & 0 \\ 0.7195 & 0.9699 & 0 \\ 0.0041 & 0.0022 & 1 \end{bmatrix} \begin{bmatrix} \Delta x_d(k) \\ y(k) \end{bmatrix} + \begin{bmatrix} 0.7195 \\ 0.4023 \\ 0.0044 \end{bmatrix} \Delta u(k) \tag{79}$$

$$A = \begin{bmatrix} 0.4872 & -0.0538 & 0 \\ 0.7195 & 0.9699 & 0 \\ 0.0041 & 0.0022 & 1 \end{bmatrix} \tag{80}$$

$$B = \begin{bmatrix} 0.7195 \\ 0.4023 \\ 0.0044 \end{bmatrix} \tag{81}$$

$$C = \begin{bmatrix} 0 & 0 & 1 \end{bmatrix} \tag{82}$$

$$D = [0] \tag{83}$$

Experiments are conducted with parameters of the control system described as follows: the initial value of the starting state variable of the system is $x_d = \begin{bmatrix} 0 & 0 \end{bmatrix}^{\mathrm{T}}$; the initial value of the starting state feedback variable of the system is $x_f = \begin{bmatrix} 0 & 0 \end{bmatrix}^{\mathrm{T}}$; the predictive time domain is $N_P = 10$; the control time domain is $N_c = 6$; the weight parameter of characteristics of the closed-loop system is $r_w = 5$; the discrete model predictive controller parameter is $K_y = 0.8388$, $K_{dmpc} = \begin{bmatrix} 0.0152 & 0.0080 & 0.8388 \end{bmatrix}$.

Figure 15 shows the experimental results within 100 predictive steps. Within 20 seconds, the output response can reach a steady state, and its coefficient of variation is 3.174%.

Conclusions

In this paper, a PI controller, the state feedback with integral controller, and the improved discrete model predictive controller have been designed by applying a roller card system and then experiments have been carried out to evaluate the quality of these controllers through web variation coefficients. Experiments indicated that the web variation coefficient of the PI controller was 4.5178% while the state feedback with integral control applied the web coefficient of variation 4.55%. In comparison with the PI controller and state feedback with integral controller,[7] the web coefficient of variation obtained from the discrete model predictive controller is 3.174%, enabling the output web to achieve better evenness. The experimental results confirmed that the carding control system with the discrete model predictive controller has the best tracking property and can apply high output response performance. Therefore, the proposed control system helps to enhance the carding efficiency and post-processing procedures.

Acknowledgement

The research was supported by the National Science Council of the Republic of China (grant number NSC 97-2221-E-011-030-MY3).

References

1. Higuchi K and Takahashi H. Automatic control of roller cards. *J Textile Machinery Soc Japan* 1964; 10: 50–58.
2. Fritzsche P. Spacing sensor arrangement and method of checking the spacing between a main carding cylinder and carding machine parts. Patent: US5040272, United States, Rieter Machine Works Limited, 1991.
3. Faas J, Naf B, Wust O, Sauter C and Gotz TG. High performance card. Patent: US6219885, United States, 2001.
4. Kuo CFJ and Hsieh TC. Dynamic analysis and control of a whole roller carding system. *Textile Res J* 2001; 71: 943.
5. Guo Y, Chen R and Hu J. Applying a generalized predictive control theory to a carding autoleveler. *Textile Res J* 2003; 73: 755–761.
6. Schlichter S and Vollrath U. Roller for a fibre-processing machine, for example a spinning preparation machine. Patent: US7578033, United States, 2009.
7. Bradley GS and Edward JK. Apparatus and method for manufacturing a multi-layer web product. Patent: US7578033, United States, 2009.
8. Schmid R and Wust O. Carding machine respectively woolen carding machine, Maschinenfavrik rieter AG. Patent: EP0989213B2, Europe, 2006.

9. Pinto A. A machine for making a non-woven fibrous web. Patent: EB177890B1. Europe, 2011.
10. Wang L. *Model predictive control system design and implementation using MATLAB*. London: Springer, 2009.
11. Huang B and Ramesh K. *Dynamic modeling predictive control and performance monitoring (Lecture Notes in Control and Information Sciences*. Vol. 374, London: Springer, 2008.
12. Kuo CFJ, Li YC and Vu QH. Quality and uniformity control of fiber web by roller card system, Part I: Dynamic modeling formulation and identification. *Textile Res J* 2012; accepted.
13. Ogata K. *Modern Control Engineering*. Englewood Cliffs, NJ: Prentice Hall, 1990.